
Inverse Reinforcement Learning by Estimating Expertise of Demonstrators

Mark Beliaev¹ Ramtin Pedarsani¹

Abstract

In Imitation Learning (IL), utilizing suboptimal and heterogeneous demonstrations presents a substantial challenge due to the varied nature of real-world data. However, standard IL algorithms consider these datasets as homogeneous, thereby inheriting the deficiencies of suboptimal demonstrators. Previous approaches to this issue typically rely on impractical assumptions like high-quality data subsets, confidence rankings, or explicit environmental knowledge. This paper introduces IRLEED, *Inverse Reinforcement Learning by Estimating Expertise of Demonstrators*, a novel framework that overcomes these hurdles without prior knowledge of demonstrator expertise. IRLEED enhances existing Inverse Reinforcement Learning (IRL) algorithms by combining a general model for demonstrator suboptimality to address reward bias and action variance, with a Maximum Entropy IRL framework to efficiently derive the optimal policy from diverse, suboptimal demonstrations. Experiments in both online and offline IL settings, with simulated and human-generated data, demonstrate IRLEED’s adaptability and effectiveness, making it a versatile solution for learning from suboptimal demonstrations.

1. Introduction

Reinforcement Learning (RL) has proven to be a versatile and powerful tool across a wide range of applications, from navigating autonomous vehicles, to playing complex games like Go and Chess. The efficacy of RL algorithms is largely attributed to their ability to optimize hand-crafted reward functions (Brockman et al., 2016). However, designing these functions is often challenging and impractical in complex environments (Hadfield-Menell et al., 2017). A prevalent alternative to this dilemma is Imitation Learning (IL), which bypasses the need for cumbersome reward

engineering by leveraging expert demonstrations to instill desired behaviors (Argall et al., 2009).

The two main approaches utilized in IL are: behavioral cloning (Pomerleau, 1991), which acquires a policy through a supervised learning approach using state-action pairs provided by the expert, and Inverse Reinforcement Learning (IRL) (Ng & Russell, 2000), which solves for the reward function that makes the expert’s behavior optimal, subsequently facilitating the training of an IL policy. Despite the effectiveness of behavior cloning in simple environments with large amounts of data, learning a policy to fit single time step decisions leads to compounding errors due to covariance shift (Ross & Bagnell, 2010). On the other hand, IRL learns a reward function that prioritizes entire trajectories over others, considering the sequential nature of the decision making problem at hand (Abbeel & Ng, 2004). Consequently, the success of IRL has spurred the development of IL techniques that either explicitly or implicitly incorporate environment dynamics (Ho & Ermon, 2016; Fu et al., 2018; Kostrikov et al., 2019; Garg et al., 2021).

However, a critical assumption in these methodologies is the availability of high-quality demonstration data. In many practical situations, especially with crowd-sourced or varied data, the quality of demonstrations is inconsistent (Mandlekar et al., 2021; Belkhale et al., 2023). For example, foundation models like GPT-3 which are trained on large and uncurated datasets, exhibit limitations such as generating biased outputs that negatively stereotype certain groups (Abid et al., 2021). In robotics, data curation becomes vital, since utilizing smaller real world datasets with noise or biases can lead to hazardous situations. Furthermore, assuming uniformity in demonstration quality overlooks the unique intentions of individual demonstrators, potentially leading to suboptimal learning outcomes (Eysenbach et al., 2018). Therefore, it is critical to develop IL methods that can account for the heterogeneity and suboptimality of demonstration data.

Addressing the challenges posed by learning from suboptimal and heterogeneous demonstrations is complex. One line of research focuses on heterogeneous demonstrations without considering their quality (Chen et al., 2020; 2023), assuming that all provided demonstrations are optimal. Other works consider suboptimal demonstrations, but require un-

¹Department of Electrical & Computer Engineering, University of California, Santa Barbara. Correspondence to: Mark Beliaev <mbeliaev@ucsb.edu>.

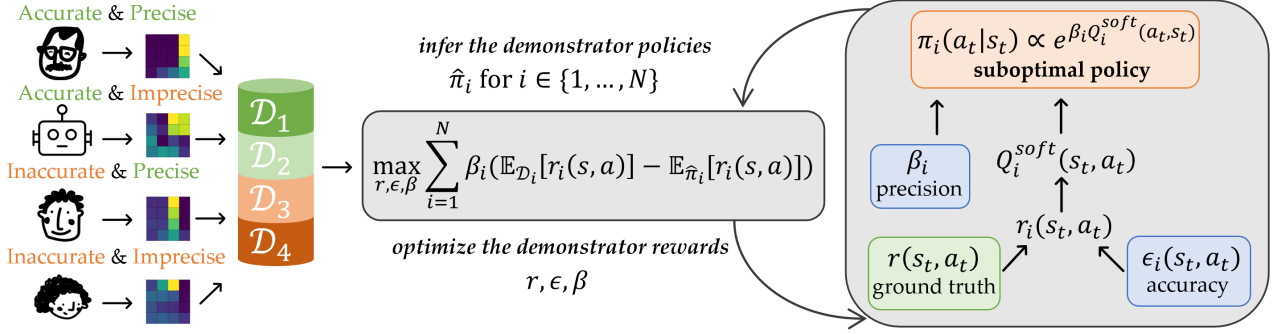


Figure 1. IRLEED can be applied in the suboptimal demonstration setting to estimate the ground truth reward r , which is used to find the optimal policy. *Left:* A heterogeneous dataset is collected from multiple sources with varying degrees of optimality. We categorize this optimality by using accuracy to represent the reward bias, and precision to represent the variance in action choices. *Right:* We can infer the demonstrator policies using a model for suboptimal behaviour based on the Boltzmann rationality principle, which captures both the accuracy ϵ_i , and the precision β_i , as compared to the ground truth reward r . *Middle:* Using estimates of the demonstrator policies $\hat{\pi}_i$ along with the demonstrations D_i , we can optimize for the true reward r , as well as the parameters that capture accuracy ϵ and precision β .

realistic prerequisites such as explicit knowledge of environment dynamics (Brown et al., 2020; Chen et al., 2021), a set of confidence scores over the demonstrations (Zhang et al., 2021; Cao & Sadigh, 2021; Wu et al., 2019; Kuhar et al., 2023), or direct access to a subset of expert demonstrations (Xu et al., 2022; Yang et al., 2021). A recently proposed approach that avoids these assumptions is ILEED (Beliaev et al., 2022), which directly models the expertise of demonstrators within a supervised learning framework, thus enabling one to learn from the optimal behavior while filtering out the suboptimal behavior of each demonstrator. While this method was proven effective, it is based on a behavioral cloning formulation, which overlooks the underlying environment dynamics, and its representation of suboptimal behavior is limited, presuming demonstrators to be noisy approximations of experts.

To overcome these challenges, this paper introduces IRLEED, *Inverse Reinforcement Learning by Estimating Expertise of Demonstrators*. As illustrated in Figure 1, IRLEED is a novel framework for IRL that accounts for demonstrator suboptimality without prior expertise knowledge. It comprises two core components: (1) a general model of demonstrator suboptimality based on the Boltzmann rationality principle, which captures both the reward bias and the variance in action choices of each demonstrator as compared to the optimal policy (2) a Maximum Entropy IRL framework, which is used to efficiently find the optimal policy when provided with a set of suboptimal and heterogeneous demonstrations. These elements enable IRLEED to effectively recover the ground truth policy from suboptimal and heterogeneous demonstrations, surpassing the limitations of previous models. Furthermore, IRLEED’s simplicity and compatibility with existing IRL techniques make it a versatile and powerful tool in the field of IL.

The main contributions of our work are:

- We propose a novel framework designed to enhance existing IRL algorithms, addressing the challenges of learning from suboptimal and heterogeneous data.
- We provide comparative insights against standard IRL and the behavior cloning approach, ILEED, showing how IRLEED generalizes both methods.
- We empirically validate the success of our method against relevant baselines in both online and offline IL scenarios, utilizing both simulated and human datasets.

2. Preliminary

Notations We consider the standard Markov decision process (MDP) setting, defined by a tuple $\mathcal{M} = (\mathcal{S}, \mathcal{A}, \mathcal{T}, p_0, r, \gamma)$, where \mathcal{S}, \mathcal{A} represent state and action spaces, $\mathcal{T} : \mathcal{S} \times \mathcal{A} \times \mathcal{S} \rightarrow [0, 1]$ represents the dynamics, $p_0 : \mathcal{S} \rightarrow [0, 1]$ represents the initial state distribution, $r \in \mathcal{R} : \mathcal{S} \times \mathcal{A} \rightarrow \mathbb{R}$ represents the reward function, and $\gamma \in (0, 1)$ represents the discount factor. In Section 3 and Section 4, we describe our method using finite state and action spaces, \mathcal{S} and \mathcal{A} , but our experiments later utilize continuous environments. We use $\pi : \mathcal{S} \times \mathcal{A} \rightarrow [0, 1]$ to denote a policy that assigns probabilities to actions in \mathcal{A} given states in \mathcal{S} . Considering the γ -discounted infinite time horizon setting, we define the expected value under a policy π in terms of the trajectory it produces. Specifically, this expectation is represented as $\bar{f}_\pi = \mathbb{E}_\pi[f(s, a)]$, which equals $\mathbb{E}[\sum_{t=0}^{\infty} \gamma^t f(s_t, a_t)]$, where $s_0 \sim p_0, a_t \sim \pi(\cdot | s_t)$, and $s_{t+1} \sim \mathcal{T}(\cdot | s_t, a_t)$. Additionally, we will use $\bar{f}_D = \mathbb{E}_D[f(s, a)]$ to denote the empirical expectation with respect to the trajectories $\tau_j = (s_0, a_0, \dots, s_T, a_T)$ in demonstration set $\mathcal{D} = \{\tau_j\}_{j=1}^M$, where we leave out denoting trajectories of varying lengths for simplicity.

Maximum Entropy IRL The goal of Inverse Reinforcement Learning (IRL) is to recover a reward $r \in \mathcal{R}$ that rationalizes the demonstrated behavior in dataset \mathcal{D} , where the provided dataset consists of trajectories τ sampled from an expert policy π_E . This general idea was first formulated as a feature-expectation matching problem (Abbeel & Ng, 2004): assuming that the feature vector $f : \mathcal{S} \times \mathcal{A} \rightarrow \mathbb{R}^k$ components quantify the expert’s behavior, to find a policy π that performs equal to or better than the expert π_E , it suffices that their feature expectations match $\bar{f}_\pi = \bar{f}_{\pi_E}$. Unfortunately, this leads to an ill-posed problem as many policies can lead to the same feature counts. Maximum Entropy IRL resolves this ambiguity by choosing the policy which does not exhibit any additional preferences beyond matching feature expectations (Ziebart et al., 2008):

$$\arg \max_{\pi} H(\pi), \text{ such that: } \bar{f}_\pi = \bar{f}_{\mathcal{D}}, \quad (1)$$

where in the infinite-time horizon setting, this equates to maximizing the discounted causal entropy $H(\pi)$ under the feature matching constraint (Bloem & Bambos, 2014).

In the MDP setting, the above problem is equivalent to finding the maximum likelihood estimate of θ :

$$\hat{\theta} = \arg \max_{\theta} \log \prod_{\tau_j \in \mathcal{D}} p_0(s_0) \prod_{t=0}^T \pi_{\theta}(a_t | s_t) \mathcal{T}(s_{t+1} | s_t, a_t), \quad (2)$$

with the parameterized policy π_{θ} defined recursively as:

$$\pi_{\theta}(a_t | s_t) = \exp(Q_{\theta}^{\text{soft}}(s_t, a_t) - V_{\theta}^{\text{soft}}(s_t)). \quad (3)$$

Here, Q^{soft} denotes the *soft* Q-function:

$$Q_{\theta}^{\text{soft}}(s_t, a_t) = \theta^{\top} f(s_t, a_t) + \gamma \mathbb{E}_{s_{t+1} \sim \mathcal{T}(\cdot | s_t, a_t)} [V_{\theta}^{\text{soft}}(s_{t+1})], \quad (4)$$

and V^{soft} denotes the *soft* Value-function:

$$V_{\theta}^{\text{soft}}(s_t) = \log \sum_{a_t \in \mathcal{A}} \exp(Q_{\theta}^{\text{soft}}(s_t, a_t)). \quad (5)$$

The parameters $\theta \in \mathbb{R}^k$ specifying the soft Bellman policy, $\pi_{\theta}(a_t | s_t)$, correspond to the dual variables of the feature matching constraint in Eq. (1). Without loss of generality, if we define the true reward signal as $r(s, a) = \theta^{*\top} f(s, a)$ for some reward parameter $\theta^* \in \mathbb{R}^k$ and features f , then the soft Bellman policy parameterized by θ^* achieves the maximum possible return (for more details see (Ziebart, 2010), Theorem 6.2 and Corollary 6.11).¹ This formulates an iterative approach to finding the true reward parameter θ^* : given demonstration set \mathcal{D} and your estimate θ , alternate between *inferring* the policy $\pi_{\theta}(a_t | s_t)$ based on Eq. (3), and *optimizing* the parameter θ based on Eq. (2).

¹To allow an arbitrary reward specification, the IRL objective defined in Eq. 1 can be expressed in terms of occupancy measures instead of feature expectations (Ho & Ermon, 2016).

This line of work provides many insights that have been used to derive modern IRL (Fu et al., 2018; Reddy et al., 2019; Gao et al., 2018; Garg et al., 2021) and RL (Haarnoja et al., 2017; 2018) algorithms. Unlike these prior works, we consider the setting where we no longer have access to the expert policy π_E , and instead are given a heterogeneous set of potentially suboptimal demonstrations from which we want to learn a well performing policy. To accomplish this, we first describe the model we use to capture the suboptimality of demonstrators in Section 3, following which we frame this problem within the IRL framework and derive our own method IRLEED in Section 4. Finally, we describe our experimental results in Section 5, and conclude our work in Section 6.

3. Suboptimal Demonstrator Model

In this work, we consider the case where dataset $\mathcal{D} = \{(i, \mathcal{D}_i)\}_{i=1}^N$ consists of a mixture of N demonstrations with varying quality. Each demonstration $\mathcal{D}_i = \{\tau_j\}_{j=1}^{M_i}$ contains a set of M_i trajectories sampled from a distinct, fixed policy π_i . Rather than considering \mathcal{D} as a homogeneous set derived from one expert policy π_E , our approach focuses on leveraging the specific source of each demonstration to enhance the IRL framework. By identifying the varying qualities within this mixed collection of demonstrations, we aim to more accurately deduce the ground truth policy π_E , as opposed to a simplistic method that averages behaviors. To achieve this, it is essential to develop a model for the demonstrators π_i that accurately reflects their suboptimal behavior relative to the optimal policy π_E .

A popular framework for modeling decision making is the Boltzmann rationality model, which is widely used in psychology (Baker et al., 2009), economics (Luce, 1959) and RL (Laidlaw & Dragan, 2021). In this model, the likelihood of an agent choosing a particular action is proportional to the exponential of the reward associated with that action: $\pi(a | s; r, \beta) \propto \exp(\beta r(s, a))$, where the inverse temperature parameter β controls the randomness of the choice. While this formulation provides an intuitive way to capture one form of suboptimality through β , it traditionally assumes that agents have unbiased knowledge about the true reward $r(s, a)$. To broaden this model for suboptimal demonstrations, we propose considering agents that follow a biased reward $r(s, a) + \epsilon(s, a)$, introducing ϵ as the deviation from the true reward. This modification enables us to represent an agent’s *accuracy* through the deviation ϵ , adding a bias to their perceived rewards, and their *precision* through parameter β , adding variance to their action choices.

Within the context of the IRL framework described in Section 2, we recall that the expert policy π_E aligns with the true reward, formulated as $r(s, a) = \theta^{*\top} f(s, a)$. Applying

the aforementioned concept, we can model a demonstrator i 's perceived reward as a deviation from the true reward: $r_i(s, a) = (\theta^* + \epsilon_i)^\top f(s, a)$, where $\epsilon_i \in \mathbb{R}^k$. By incorporating this altered reward r_i into the *soft* Bellman policy defined in Eq. (3), we derive a recursive parameterization for demonstrator i 's policy:

$$\pi_{\theta^*, \epsilon_i, \beta_i}(a_t | s_t) \propto \exp(\beta_i(Q_{\theta^* + \epsilon_i}^{\text{soft}}(s_t, a_t))), \quad (6)$$

where $\beta_i \in [0, \infty)$, and the normalizing factor not shown above should be modified to account for β_i : $V_{\theta^* + \epsilon_i}^{\text{soft}}(s_t) = \frac{1}{\beta_i} \log \sum_{a_t \in \mathcal{A}} \exp(\beta_i Q_{\theta^* + \epsilon_i}^{\text{soft}}(s_t, a_t))$.

Our model captures two distinct aspects of suboptimal behavior: (1) ϵ_i quantifies the demonstrator's *accuracy* in estimating the true reward r , where $\epsilon_i^\top f(\tau)$ represents the estimation error. (2) β_i quantifies the demonstrator's *precision* in action selection, where $\beta_i \rightarrow \infty$ interpolates from the soft Bellman policy, which samples actions according to their Q-values, to the standard Bellman policy, which chooses actions that maximize the Q-value. This model offers a versatile and mathematically convenient way to depict suboptimal demonstrator behaviors within the soft Bellman policy domain, as well as extend the results of Maximum Causal Entropy IRL to the suboptimal setting.

Remark 3.1. *Before moving forward, it is important to note that this model extends outside the scope of problems where the true reward r is an affine transformation of some feature vector f . In the general setting, we can parameterize demonstrator i 's reward as $r_i = r + \epsilon_i$, a combination of the true reward $r \in \mathcal{R}$ and their deviation $\epsilon_i \in \mathcal{R}$, where r and ϵ_i can be represented by neural networks to allow for general function approximation. We opt to formulate our proposed model within the classic feature matching scope, as this facilitates direct comparison with the seminal works used to derive our results in the following section. However, our proposed model's applicability extends beyond this traditional framework, as we elaborate in Section 4.3, and demonstrate through experiments in Section 5. Until then, we utilize the feature matching framework described, referencing it as standard IRL.*

4. Learning from Suboptimal Data with IRL

Up to this point, we have formulated a model for each demonstrator i based on the parameter θ^* , which defines the true reward, and parameters ϵ_i and β_i , which characterize demonstrator suboptimalities. However, we do not have access to any of these parameters, and are instead provided with a dataset of demonstrations \mathcal{D} . Recall that standard IRL assumes that all demonstrations come from the optimal policy π_E , and follows the iterative approach described in Section 2 to find it. However, applying this approach to the heterogeneous regime will yield an averaged policy, which can lead to subpar performance if a significant portion of

the provided demonstrations are suboptimal.

To refine this, we introduce IRLEED, an innovative extension of the IRL framework tailored for the suboptimal setting. Firstly, Section 4.1 details how IRLEED extends the standard IRL framework, which corresponds to the predefined feature matching setting. Following this, Section 4.2 presents insightful comparisons between our IRLEED approach and the standard IRL framework, along with the related behavior cloning approach, ILEED. Finally, Section 4.3 explains how IRLEED can be applied to the generalized IRL setting, addressing the practical considerations necessary for implementing our framework in conjunction with existing IRL methodologies.

4.1. IRLEED

Utilizing the dataset $\mathcal{D} = \{(i, \mathcal{D}_i)\}_{i=1}^N$, we can jointly estimate the unknown parameters by maximizing the likelihood defined below:

$$\mathcal{L}(\theta, \epsilon, \beta) = \log \prod_{\mathcal{D}_i \in \mathcal{D}} \prod_{\tau_j \in \mathcal{D}_i} P(\tau_j | \theta, \epsilon_i, \beta_i), \quad (7)$$

where $\epsilon = \{\epsilon_i\}_{i=1}^N$, $\beta = \{\beta_i\}_{i=1}^N$, and the probability $P(\tau_j | \theta, \epsilon_i, \beta_i)$ is given by:

$$P(\tau | \theta, \epsilon_i, \beta_i) = p_0(s_0) \prod_{t=0}^T \pi_{\theta, \epsilon_i, \beta_i}(a_t | s_t) \mathcal{T}(s_{t+1} | s_t, a_t). \quad (8)$$

Under the specified demonstrator model, this likelihood serves as a suitable loss function. Specifically, rewriting the joint likelihood equivalently only over θ :

$$\mathcal{L}(\theta) = \max_{\epsilon, \beta} \mathcal{L}(\theta, \epsilon, \beta), \quad (9)$$

it is easy to show that $\mathcal{L}(\theta)$ is a proper objective function.

Proposition 4.1. θ^* is the (non-unique) maximizer of $\mathcal{L}(\theta)$.

Moreover, this formulation provides us with a convenient way to derive the gradient of likelihood function $\mathcal{L}(\theta, \epsilon, \beta)$.

Lemma 4.2. *Given the likelihood \mathcal{L} defined according to Eq. (7) and demonstrator policies $\pi_{\theta, \epsilon_i, \beta_i}$ parameterized by Eq. (6), we can compute the gradients of \mathcal{L} as follows:*

$$\nabla_{\theta} \mathcal{L} = \sum_{i=1}^N \beta_i (\tilde{f}_{\mathcal{D}_i} - \bar{f}_{\pi_{\theta, \epsilon_i, \beta_i}}), \quad (10)$$

$$\nabla_{\epsilon_i} \mathcal{L} = \beta_i (\tilde{f}_{\mathcal{D}_i} - \bar{f}_{\pi_{\theta, \epsilon_i, \beta_i}}), \quad (11)$$

$$\frac{\partial \mathcal{L}}{\partial \beta_i} = (\theta + \epsilon_i)^\top (\tilde{f}_{\mathcal{D}_i} - \bar{f}_{\pi_{\theta, \epsilon_i, \beta_i}}). \quad (12)$$

Proof. First, note that parameter β_i can be folded inside the modified *soft* Bellman policy of Eq. (6) as the reward estimate: $\beta_i(\theta + \epsilon_i)^\top f(s_t, a_t)$. Second, we can

express the likelihood as $\mathcal{L} = \sum_{i=1}^N \mathcal{L}_i$, where $\mathcal{L}_i = \log \prod_{\tau_j \in \mathcal{D}_i} P(\tau_j | \theta, \epsilon_i, \beta_i)$. Setting $u_i = \beta_i(\theta + \epsilon_i)$, we know that $\nabla_{u_i} \mathcal{L}_i = \tilde{f}_{\mathcal{D}_i} - \bar{f}_{\pi_{\theta, \epsilon_i, \beta_i}} \forall i \in \{1, \dots, N\}$ (see (Ziebart, 2010), Theorem 6.2 and Lemma A.2). Applying the chain rule completes the proof. \square

Notably, this result has an intuitive interpretation. Recall that for each demonstrator i , $\tilde{f}_{\mathcal{D}_i} - \bar{f}_{\pi_{\theta, \epsilon_i, \beta_i}}$ represents the difference between the empirical feature vector given samples from their policy, $\tilde{f}_{\mathcal{D}_i}$, and the expected feature vector under the probabilistic model, $\bar{f}_{\pi_{\theta, \epsilon_i, \beta_i}}$. With this in mind, Eq. (11) shows that we update ϵ_i to directly match feature expectation with demonstrator π_i , just like in standard IRL. On the other hand, Eq. (10) shows that we update θ to match a weighted average over feature expectations provided by all demonstrators, where their respective precision β_i determines their contribution. Finally, Eq. (12) shows that we update this precision β_i to balance the expected returns of the demonstrator, π_i , and our probabilistic model, $\pi_{\theta, \epsilon_i, \beta_i}$, under our estimate of the perceived reward, $r_i(s, a) = (\theta + \epsilon_i)^\top f(s, a)$. This way, when the probabilistic model outperforms the demonstration set under the estimated reward r_i , we decrease the precision β_i to lower its relative performance, and vice versa.

The above formulation gives us a general algorithm that extends the IRL framework described in Section 2. Specifically, IRLEED follows an iterative approach to finding the true reward parameter θ^* : given demonstration set $\mathcal{D} = \{(i, \mathcal{D}_i)\}_{i=1}^N$ and estimates θ, ϵ, β , for each demonstrator $i \in \{1, \dots, N\}$, alternate between *inferring* the policy $\pi_{\theta, \epsilon_i, \beta_i}(a_t | s_t)$ based on Eq. (6), and *optimizing* the parameters $\theta, \epsilon_i, \beta_i$ based on Eqs. (10), (11), (12), respectively.

As aforementioned, many different techniques can be used for both the inference and optimization procedures. For example, to infer the policy $\pi_{\theta, \epsilon_i, \beta_i}(a_t | s_t)$ given $\theta, \epsilon_i, \beta_i$, one can use soft versions of the standard value iteration and Q-learning algorithms depending on whether the dynamics \mathcal{T} are provided or not (Bloem & Bambos, 2014). To compute feature expectations $\bar{f}_{\pi_{\theta, \epsilon_i, \beta_i}}$ based on the inferred policy, one can directly compute the expectations by utilizing the standard dynamic programming operator when the dynamics \mathcal{T} are known, or estimate the expectations by utilizing Monte Carlo simulations of the MDP when the dynamics \mathcal{T} are unknown.

4.2. Comparisons to Standard IRL and ILEED

We can see that this likelihood maximization problem is closely related to the maximum causal entropy IRL framework described in Eqs. (1)-(5). Specifically, IRLEED makes two modification: (1) For each $i \in \{1, \dots, N\}$, it defines individual dual variables $\theta_i = \theta + \epsilon_i$ that correspond to feature matching constraint $\tilde{f}_{\mathcal{D}_i} = \bar{f}_{\pi_{\theta, \epsilon_i, \beta_i}}$, tying

the demonstrator policies together. (2) It uses a learnable parameter β_i to tune the magnitude of uncertainty related to demonstrations provided in \mathcal{D}_i . Moreover, IRLEED generalizes the standard IRL framework.

Remark 4.3. *IRLEED recovers the standard IRL framework when we set $\epsilon_i = [0]^k$ and $\beta_i = 1$ as constants.*

To show the advantage of IRLEED within the suboptimal demonstration setting, we note that the policy recovered by standard IRL can only perform as well as the average demonstration \mathcal{D}_i provided. This is a direct result of the feature matching constraint imposed by the IRL objective.

Proposition 4.4. *Given demonstrations $\mathcal{D} = \{(i, \mathcal{D}_i)\}_{i=1}^N$ produced by suboptimal policies π_i defined according to Eq. (6), let θ_{IRL} denote the naive solution to the standard IRL problem defined by Eq. 2, which treats demonstration set \mathcal{D} as one homogeneous set produced by π_E . The performance of IRL is bounded by:*

$$\mathbb{E}_{\pi_{\theta_{IRL}}} [r(s, a)] = \frac{1}{N} \sum_{i=1}^N \mathbb{E}_{\pi_i} [r(s, a)] \leq \mathbb{E}_{\pi_{\theta^*}} [r(s, a)], \quad (13)$$

where for simplicity, we assume that all demonstrators provide the same number of trajectories $M_i = M$.

As mentioned in Proposition 4.1, IRLEED can recover the true reward parameter θ^* , which outperforms θ_{IRL} unless the demonstrations provided are optimal. Unfortunately, since θ^* is not the unique solution to IRLEED, we can not make guarantees on recovering the true reward parameter θ^* . Nonetheless, our experimental results in Section 5 demonstrate that IRLEED improves performance over IRL frameworks in both the feature matching setting described here, as well as more complex scenarios which include high dimensional input spaces and human demonstrations.

Finally, we note that when the MDP is deterministic, we can express the policy without recursion:

$$\pi_{\theta, \epsilon_i, \beta_i}(\tau) \propto \exp(\beta_i(\theta + \epsilon_i)^\top f(\tau)), \quad (14)$$

where $f(\tau) = \sum_{(s,a) \in \tau} f(s, a)$, and $\pi(\tau)$ can directly map from trajectories due to the deterministic dynamics \mathcal{T} . Replacing the probability $P(\tau | \theta, \epsilon_i, \beta_i)$ with $\pi_{\theta, \epsilon_i, \beta_i}(\tau)$, we can see that maximizing the likelihood defined by Eq. (7) corresponds to the supervised learning approach employed by ILEED (Beliaev et al., 2022).

Remark 4.5. *IRLEED recovers the ILEED framework if we assume all demonstrators i have full knowledge of the true reward, $\epsilon_i = [0]^k$, and ignore the underlying dynamics of the MDP.*

Hence unlike ILEED, our framework provides us with a dynamics-aware solution to the problem of learning from mixtures of suboptimal demonstrations. As we demonstrate

in Section 5, IRLEED can be utilized offline to achieve superior performance compared to ILEED.

4.3. Extension to Generalized IRL

While the results in the previous sections provide insight on how to learn from suboptimal demonstrations using IRL, relying on hand-crafted features f can hinder our ability to express complex behavior. In general, the true reward r can belong to a non restrictive set of functions $\mathcal{R} = \{r : \mathcal{S} \times \mathcal{A} \rightarrow \mathbb{R}\}$. In this case, one can utilize the generalized IRL objective instead:

$$\max_{r \in \mathcal{R}} \min_{\pi \in \Pi} \mathbb{E}_{\pi_E} [r(s, a)] - \mathbb{E}_{\pi} [r(s, a)] - H(\pi) - \psi(r), \quad (15)$$

where ψ is a convex reward regularizer that smoothly penalizes differences between occupancy measures to prevent overfitting (Ho & Ermon, 2016). A naive solution to this nested min-max objective involves an outer loop learning the reward, and an inner loop executing maximum entropy RL with this reward to find the optimal policy. As before, the optimal policy under reward r takes the form of the soft Bellman policy defined in Equation (3), where $r(s, a)$ replaces the linear reward $\theta^\top f(s, a)$. The description of IRLEED in the generalized setting follows directly.

Since the suboptimal demonstrator model defined in Equation (6) extends to this setting, we can parameterize our estimate of demonstrator i 's policy with the soft Bellman policy $\hat{\pi}_i$ under the reward estimate $r_i = r + \epsilon_i$ and precision β_i . Utilizing the dataset $\mathcal{D} = \{(i, \mathcal{D}_i)\}_{i=1}^N$, the outer loop of the generalized IRLEED objective is simplified to:

$$\max_{r, \epsilon, \beta} \sum_{i=1}^N \beta_i (\mathbb{E}_{\mathcal{D}_i} [r_i(s, a)] - \mathbb{E}_{\hat{\pi}_i} [r_i(s, a)]) - \psi(\beta_i r_i), \quad (16)$$

where in practice, the unknown functions r and $\epsilon = \{\epsilon_i\}_{i=1}^N$ can be parameterized by neural networks. Note that under a constant reward regularizer ψ , if we express the rewards as $r_i(s, a) = (\theta + \epsilon_i)^\top f(s, a)$, then the gradients of the above objective are identical to the ones described in Lemma 4.2.

In summary, we have shown how any learning algorithm that solves the generalized IRL objective defined in Equation (15) can be utilized alongside our framework by reparameterizing the reward and policy accordingly. Our experiment results in Section 5 demonstrate that IRLEED performs well in this generalized setting, and can even be trained offline when paired with Inverse soft-Q learning (IQ), an approach that avoids the iterative process defined by learning a single Q-function, implicitly representing both reward and policy (Garg et al., 2021).

5. Experiments

In this section, we empirically evaluate how IRLEED performs when learning from suboptimal demonstrations, using

experiments in both online and offline IL settings, with simulated and human-generated data. In total, we performed three sets of experiments, comparing IRLEED to maximum entropy IRL (Ziebart et al., 2010), Inverse soft-Q learning (IQ) (Garg et al., 2021), and ILEED (Beliaev et al., 2022). We go over the results of each experiment below, briefly detailing the corresponding setup for each. For further implementation details refer to Appendix A.

5.1. Gridworld

For our first experiment, we used a custom gridworld environment, simulating suboptimal demonstrations with varying levels of *precision* and *accuracy*. Using this environment, we compared the performance of IRLEED against maximum entropy IRL.

Setup The reward in this setting was linearly parameterized as $r(s) = \theta^\top f(s)$, where $f(s)$ is simply a one hot encoding for each gridworld state. To implement IRL, we utilized stochastic value iteration on the reward estimate θ to infer the policy π , and Monte Carlo simulations of the MDP to estimate the feature expectations required to optimize θ , repeating both steps until convergence. We used the same processes to implement IRLEED according to the procedure outlined in Section 4, updating ϵ and β only after θ converged, and repeating this for two iterations.

For each level of *precision* and *accuracy*, we randomly generated 5 suboptimal policies according to Equation (6), where β_i was sampled from a uniform distribution starting at 0, with mean equal to the *precision* level, and ϵ_i was sampled from a multivariate normal distribution $\mathcal{N}([0]^k, \mathbf{I}_k/\lambda^2)$, with λ equal to the *accuracy* level. We tested a total of 121 dataset settings, collecting 40 trajectories from each policy to compose our dataset, and comparing the performance of IRLEED and IRL over 100 seeds for each setting.

Results We first compare how IRLEED and IRL recover the reward $r(s, a)$ when provided with suboptimal demonstrations. We visualize the averaged result for one dataset setting in Figure 2, which shows the true reward, the dataset quality, and the recovered rewards under both methods. We can see that the provided demonstrations are misaligned with the ground truth reward: the state visitation frequency for the top left corner is higher due to demonstrator suboptimality. As expected, the feature matching constraint of IRL absorbs this suboptimality. Although the reward recovered by IRL contains information about the true reward, it is now incorrectly biasing the top left corner. On the other hand, IRLEED is able to remove this bias, providing us with a better estimate of the ground truth reward.

To see the effect of dataset quality, we use Figure 3 to show the relative improvement of the policy recovered by IRLEED over maximum entropy IRL for each dataset set-

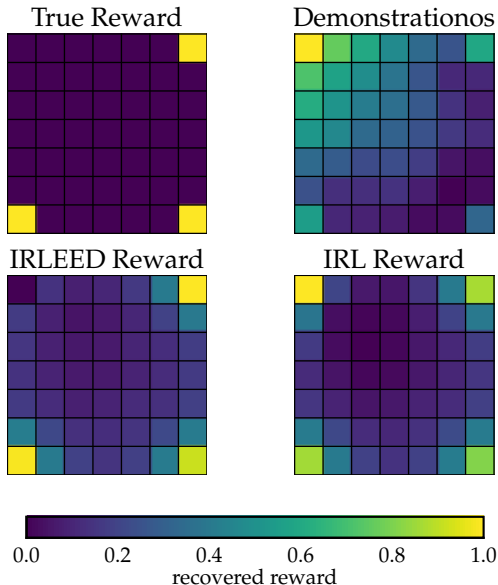


Figure 2. We visualize the reward recovered by IRLEED and IRL when trained using suboptimal demonstrations. Top left shows the true reward, where the three yellow corners are terminal states. Top right shows the normalized state visitation frequency over the entire dataset. Bottom left and right show the normalized rewards recovered by IRLEED and IRL respectively.

ting. We can see from the left plot that IRLEED provides more improvement over IRL as we decrease accuracy ϵ (by decreasing λ), or increase precision β . This signifies the importance of modeling the precision ϵ , or reward bias, in addition to the accuracy β , or action variance, when learning from suboptimal demonstrations. This point is further highlighted in the right plot, which shows that although both IRLEED and IRL suffer when demonstrator accuracy is diminished, IRLEED can tolerate lower demonstrator accuracy compared to IRL. In total, IRLEED provided a 30.3% improvement over IRL for the 121 settings tested.

5.2. Simulated Control Tasks

For our second experiment, we used two control tasks, Cartpole, and Lunar Lander, simulating suboptimal demonstrations with varying levels of *expertise* and *accuracy*. Using these two environments, we compared the performance of IRLEED, IQ, and ILEED in both the online and offline settings.

Setup To implement IQ, and setup the training and evaluation procedures, we utilized the codebase provided by the authors. We implemented ILEED alongside this codebase, using the training and evaluation procedures. For IRLEED, we built on top of the aforementioned IQ implementation by adding a learnable parameter β_i , and an additional critic

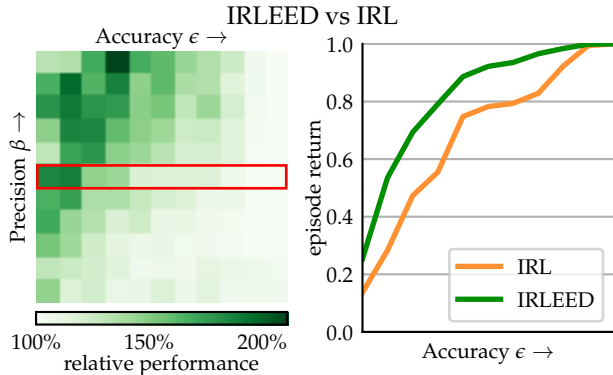


Figure 3. We compare the performance of the policies recovered by IRLEED and IRL. The left plot shows the relative performance of IRLEED over IRL under varying dataset settings, where the top right corner corresponds to expert data. The right plot shows the performance of both policies as we increase the average accuracy ϵ of demonstrators in the dataset, corresponding to the data outlined in red in the left plot.

network ϵ_i , for each demonstrator i . Since IQ learns a reward and policy directly by using a single Q function as a critic, we used our additional critic network ϵ_i to directly add bias to the state action function instead of the reward.

For this experiment, we used 4 dataset settings corresponding to the *precision* and *accuracy* levels: (high, high), (high, low), (low, high), and (low, low). For each setting, we randomly generated 3 suboptimal policies according to $\pi_i(a|s) \propto \exp(\beta_i(Q(s, a) + \alpha\epsilon_i(s, a)))$, where $Q(s, a)$ is a pretrained critic network, $\epsilon_i(s, a)$ is a randomly initialized critic network, and α is a scaling factor which is set to zero for the high *accuracy* setting. For the low *precision* setting, β_i was sampled from a uniform distribution, whereas for the high *precision* setting, the stochasticity of the policy was removed by following the maximum state action value. We ran this experiment in both the online and offline setting, comparing the performance of IRLEED, IQ, and ILEED, using 30 seeds for each dataset setting.

Results We first compare how IRLEED improves over IQ, with online access to environment interactions. We provide these results in Tables 1 and 2, which show the return of the recovered policy relative to the return of the best demonstrator in that dataset. We can see that IRLEED outperforms its ablated counterpart, IQ, under all 3 suboptimal dataset settings (not including the clean dataset), for both environments. Furthermore, we see that in the more complex Lunar Lander environment, IQ can not perform as well as the best demonstrator, whereas IRLEED consistently performs on par or better than the best demonstrator.

To have a fair comparison between IRLEED and its behaviour cloning counterpart, ILEED, we repeat these exper-

Table 1. Cartpole

We list the average return of the recovered policies (IQ, IRLEED, ILEED), relative to the return of the best demonstrator. This is provided for 4 dataset settings (Prec., Acc.), where we list the mean performance of all demonstrators relative to the best demonstrator (Mean). The last row (H,H) corresponds to a clean dataset. The return of the best demonstrator corresponding to each setting (top to bottom) is: 260, 500, 411, 500.

Setting			Online		Offline		
Prec.	Acc.	Mean	IQ	IRLEED	ILEED	IQ	IRLEED
<i>L</i>	<i>L</i>	0.58	0.97	1.55	1.38	0.96	1.56
<i>L</i>	<i>H</i>	0.70	0.92	1.00	1.00	0.96	1.00
<i>H</i>	<i>L</i>	0.64	1.03	1.09	1.05	0.95	1.05
<i>H</i>	<i>H</i>	1.00	0.99	1.00	0.92	1.00	1.00

iments without online access to environment interactions. Firstly, we can see that from Tables 1 and 2 that offline IRLEED outperforms ILEED, under all 3 suboptimal dataset settings, for both environments. We can see that although ILEED has comparable performance in the simpler Cartpole environment, it performs poorly in the more complex Lunar Lander environment. Moreover, we can see from Table 2 that ILEED shows diminished performance when demonstrators have low accuracy ϵ , signifying that it can not account for the reward biases present in these settings.

5.3. Atari with Human Data

For our final experiment, we used two Atari environments, Space Invaders, and Qbert, utilizing both simulated and human demonstrations. Using these two environments, we compared the performance of IRLEED, IQ, and ILEED in the offline setting.

Setup Our demonstrations were comprised of two unique sources, dataset *A*: simulated data using a pretrained expert policy and dataset *B*: collected data using adept human players (Kurin et al., 2017). Since the human dataset *B* was acquired using screenshots of web-browsers, there is a small mismatch in sampling frequencies and colors when compared to the simulated environment used in dataset *A*. This provides a unique challenge akin to crowd-sourcing data from varying sources, where the goal is to see if we can achieve improved performance when training on the

Table 2. Lunar Lander

See Table 1. The return of the best demonstrator corresponding to each setting (top to bottom) is: 171, 213, 166, 277.

Setting			Online		Offline		
Prec.	Acc.	Mean	IQ	IRLEED	ILEED	IQ	IRLEED
<i>L</i>	<i>L</i>	0.46	0.68	1.28	0.84	0.81	1.34
<i>L</i>	<i>H</i>	0.54	0.84	1.14	1.06	1.05	1.18
<i>H</i>	<i>L</i>	0.57	0.94	1.30	0.85	0.99	1.14
<i>H</i>	<i>H</i>	0.86	0.93	0.98	1.01	0.99	0.98

Table 3. Utilizing Demonstrations from Varying Sources

We list the average return of the recovered policies (IQ, IRLEED, ILEED). This is provided for 3 dataset settings, simulated dataset *A*, human dataset *B* (Kurin et al., 2017), and their combination *AB*. Overall we see IRLEED shows a 16% improvement over IQ, and a 41% improvement over ILEED in the combined *AB* setting.

Dataset	Space Invaders			Qbert		
	ILEED	IQ	IRLEED	ILEED	IQ	IRLEED
<i>AB</i>	802	755	910	5511	8248	9336
<i>A</i>	783	754	768	5926	8092	8049
<i>B</i>	110	179	123	0	809	1087

combined dataset *AB* as opposed to dataset *A* alone. Note that we followed the same steps outlined in the previous Section 5.2 to implement the three methods and setup the training and evaluation procedures. The results shown are averaged over 5 seeds.

Results With this setup, we would like to test if IRLEED can improve the crowd-sourcing capability of IQ, and compare its performance to ILEED. We provide these results for both environments in Table 3, which lists the return of the recovered policies. Notably, all methods do poorly when trained exclusively on dataset *B*, due to the mismatch between the simulation environment and the data. On the other hand, utilizing dataset *A* is enough to reach decent performance. However, we can see that IRLEED is the only method that significantly improves its performance when utilizing the combined dataset *AB* as opposed to dataset *A*.

6. Discussion

In summary, this paper addresses the challenges of leveraging suboptimal and heterogeneous demonstrations in IL by introducing IRLEED, a novel IRL framework. By integrating a general model of demonstrator suboptimality that accounts for reward bias and action variance, with a maximum entropy IRL framework, IRLEED successfully mitigates the limitations inherent in standard IL algorithms, which often fail to account for the diversity and imperfections in real-world data. We empirically demonstrate that IRLEED can be used alongside existing IRL techniques to improve their performance in the presence of suboptimal and heterogeneous demonstrations. Moreover, we show that IRLEED outperforms its behavior cloning counterpart ILEED in the offline setting, demonstrating the importance of utilizing a dynamics-aware approach that considers reward bias. Although we have shown that IRLEED improves over IRL in a multitude of settings, we have not provided guarantees that state whether IRLEED will recover a better reward estimate compared to IRL. One direction for future work could be to provide more theoretical analysis comparing IRLEED to IRL under simpler settings with strict assumptions.

7. Impact Statement

This paper presents work whose goal is to advance the field of Machine Learning. There are many potential societal consequences of our work, none which we feel must be specifically highlighted here.

References

- Abbeel, P. and Ng, A. Y. Apprenticeship learning via inverse reinforcement learning. In *Proceedings of the twenty-first international conference on Machine learning*, pp. 1, 2004.
- Abid, A., Farooqi, M., and Zou, J. Large language models associate muslims with violence. *Nature Machine Intelligence*, 3(6):461–463, 2021.
- Argall, B. D., Chernova, S., Veloso, M., and Browning, B. A survey of robot learning from demonstration. *Robotics and autonomous systems*, 57(5):469–483, 2009.
- Baker, C. L., Saxe, R., and Tenenbaum, J. B. Action understanding as inverse planning. *Cognition*, 113(3):329–349, 2009.
- Beliaev, M., Shih, A., Ermon, S., Sadigh, D., and Pedarsani, R. Imitation learning by estimating expertise of demonstrators. In *International Conference on Machine Learning*, pp. 1732–1748. PMLR, 2022.
- Belkhale, S., Cui, Y., and Sadigh, D. Data quality in imitation learning. *arXiv preprint arXiv:2306.02437*, 2023.
- Bloem, M. and Bambos, N. Infinite time horizon maximum causal entropy inverse reinforcement learning. In *53rd IEEE Conference on Decision and Control*, pp. 4911–4916, 2014. doi: 10.1109/CDC.2014.7040156.
- Brockman, G., Cheung, V., Pettersson, L., Schneider, J., Schulman, J., Tang, J., and Zaremba, W. Openai gym, 2016.
- Brown, D. S., Goo, W., and Niekum, S. Better-than-demonstrator imitation learning via automatically-ranked demonstrations. In *Conference on robot learning*, pp. 330–359. PMLR, 2020.
- Cao, Z. and Sadigh, D. Learning from imperfect demonstrations from agents with varying dynamics. *IEEE Robotics and Automation Letters*, 6(3):5231–5238, 2021.
- Chen, L., Paleja, R., Ghuy, M., and Gombolay, M. Joint goal and strategy inference across heterogeneous demonstrators via reward network distillation. In *Proceedings of the 2020 ACM/IEEE international conference on human-robot interaction*, pp. 659–668, 2020.
- Chen, L., Paleja, R., and Gombolay, M. Learning from sub-optimal demonstration via self-supervised reward regression. In *Conference on robot learning*, pp. 1262–1277. PMLR, 2021.
- Chen, L., Jayanthi, S., Paleja, R. R., Martin, D., Zakharov, V., and Gombolay, M. Fast lifelong adaptive inverse reinforcement learning from demonstrations. In *Conference on Robot Learning*, pp. 2083–2094. PMLR, 2023.
- Eysenbach, B., Gupta, A., Ibarz, J., and Levine, S. Diversity is all you need: Learning skills without a reward function. In *International Conference on Learning Representations*, 2018.
- Fu, J., Luo, K., and Levine, S. Learning robust rewards with adversarial inverse reinforcement learning. In *International Conference on Learning Representations*, 2018.
- Gao, Y., Xu, H., Lin, J., Yu, F., Levine, S., and Darrell, T. Reinforcement learning from imperfect demonstrations. *arXiv preprint arXiv:1802.05313*, 2018.
- Garg, D., Chakraborty, S., Cundy, C., Song, J., and Ermon, S. Iq-learn: Inverse soft-q learning for imitation. *Advances in Neural Information Processing Systems*, 34: 4028–4039, 2021.
- Haarnoja, T., Tang, H., Abbeel, P., and Levine, S. Reinforcement learning with deep energy-based policies. In *International conference on machine learning*, pp. 1352–1361. PMLR, 2017.
- Haarnoja, T., Zhou, A., Abbeel, P., and Levine, S. Soft actor-critic: Off-policy maximum entropy deep reinforcement learning with a stochastic actor. In *International conference on machine learning*, pp. 1861–1870. PMLR, 2018.
- Hadfield-Menell, D., Milli, S., Abbeel, P., Russell, S. J., and Dragan, A. Inverse reward design. *Advances in neural information processing systems*, 30, 2017.
- Ho, J. and Ermon, S. Generative adversarial imitation learning. *Advances in neural information processing systems*, 29, 2016.
- Kostrikov, I., Nachum, O., and Tompson, J. Imitation learning via off-policy distribution matching. In *International Conference on Learning Representations*, 2019.
- Kuhar, S., Cheng, S., Chopra, S., Bronars, M., and Xu, D. Learning to discern: Imitating heterogeneous human demonstrations with preference and representation learning. In Tan, J., Toussaint, M., and Darvish, K. (eds.), *Proceedings of The 7th Conference on Robot Learning*, volume 229 of *Proceedings of Machine Learning Research*, pp. 1437–1449. PMLR, 06–09 Nov

2023. URL <https://proceedings.mlr.press/v229/kuhar23a.html>.
- Kurin, V., Nowozin, S., Hofmann, K., Beyer, L., and Leibe, B. The atari grand challenge dataset. *arXiv preprint arXiv:1705.10998*, 2017.
- Laidlaw, C. and Dragan, A. The boltzmann policy distribution: Accounting for systematic suboptimality in human models. In *International Conference on Learning Representations*, 2021.
- Luce, R. D. Individual choice behavior. 1959.
- Mandlekar, A., Xu, D., Wong, J., Nasiriany, S., Wang, C., Kulkarni, R., Fei-Fei, L., Savarese, S., Zhu, Y., and Martín-Martín, R. What matters in learning from off-line human demonstrations for robot manipulation. In *Conference on robot learning*, 2021.
- Ng, A. Y. and Russell, S. J. Algorithms for inverse reinforcement learning. In *Proceedings of the Seventeenth International Conference on Machine Learning*, pp. 663–670, 2000.
- Pomerleau, D. A. Efficient training of artificial neural networks for autonomous navigation. *Neural computation*, 3(1):88–97, 1991.
- Reddy, S., Dragan, A. D., and Levine, S. Sqil: Imitation learning via reinforcement learning with sparse rewards. In *International Conference on Learning Representations*, 2019.
- Ross, S. and Bagnell, D. Efficient reductions for imitation learning. In *Proceedings of the thirteenth international conference on artificial intelligence and statistics*, pp. 661–668. JMLR Workshop and Conference Proceedings, 2010.
- Wu, Y.-H., Charoenphakdee, N., Bao, H., Tangkaratt, V., and Sugiyama, M. Imitation learning from imperfect demonstration. In *International Conference on Machine Learning*, pp. 6818–6827. PMLR, 2019.
- Xu, H., Zhan, X., Yin, H., and Qin, H. Discriminator-weighted offline imitation learning from suboptimal demonstrations. In *International Conference on Machine Learning*, pp. 24725–24742. PMLR, 2022.
- Yang, M., Levine, S., and Nachum, O. Trail: Near-optimal imitation learning with suboptimal data. In *International Conference on Learning Representations*, 2021.
- Zhang, S., Cao, Z., Sadigh, D., and Sui, Y. Confidence-aware imitation learning from demonstrations with varying optimality. *Advances in Neural Information Processing Systems*, 34:12340–12350, 2021.
- Ziebart, B. D. *Modeling purposeful adaptive behavior with the principle of maximum causal entropy*. Carnegie Mellon University, 2010.
- Ziebart, B. D., Maas, A., Bagnell, J. A., and Dey, A. K. Maximum entropy inverse reinforcement learning. In *Proceedings of the 23rd national conference on Artificial intelligence-Volume 3*, pp. 1433–1438, 2008.
- Ziebart, B. D., Bagnell, J. A., and Dey, A. K. Modeling interaction via the principle of maximum causal entropy. 2010.

A. Implementation Details

Below we detail the experimental setups utilized in Section 5, and provide information on the computational resources used for our work. Note that we provide a working implementation of the Gridworld experiments found in Section 5.1 as part of our supplementary material, and plan to release a public implementation of IRLEED with all experiments and datasets used after publication.

A.1. Gridworld

To implement both IRLEED and IRL for the Gridworld experiments in Section 5.1, we utilized stochastic value iteration on the reward estimate θ to infer the policy π , and Monte Carlo simulations of the MDP to estimate the feature expectations required to optimize θ , repeating both steps until convergence. As stated, when using IRLEED, we only updated ϵ and β after θ converged, and repeated this for two iterations. For stochastic value iteration, we used a discount factor of 0.9, a maximum horizon of 100 timesteps, and a convergence criteria of $1e - 4$ on the inferred state action values. For Monte Carlo simulations, we used 100 episode samples. For optimization, we used stochastic gradient ascent with learning rates of 0.05, 0.1, 0.2 for β , ϵ , θ , respectively, and a convergence criteria of $1e - 4$ on θ . For IRL, we initialized $\theta = [0.1]^k$, and set $\beta_i = 1$ and $\epsilon_i = [0]^k$ to constants for all demonstrators, removing their effect. For evaluation, we used the policy recovered from the final estimate of θ , sampling 100 episodes to measure the mean reward.

To create datasets for varying levels of *precision* and *accuracy*, we randomly generated 5 suboptimal policies according to Equation (6), where β_i was sampled from a uniform distribution starting at 0, with mean equal to the *precision* level, and ϵ_i was sampled from a multivariate normal distribution $\mathcal{N}([0]^k, \mathbf{I}_k/\lambda^2)$, with λ equal to the *accuracy* level. For β , the maximum values used for the uniform distribution were: 0.4, 0.5, 1, 1.5, 2, 2.5, 3, 3.5, 4, 4.5, 5. For λ , the values used were: 2, 2.5, 3, 3.5, 4, 4.5, 5, 5.5, 6, 10, ∞ , where ∞ corresponds to setting $\epsilon_i = [0]^k$ to remove its effect. We tested a total of 121 dataset settings, collecting 40 trajectories from each policy to compose our dataset, and comparing the performance of IRLEED and IRL over 100 seeds for each setting.

A.2. Simulated Control Tasks

To implement IQ and setup the training and evaluation procedures for the simulated control tasks in Section 5.2, we utilized the codebase provided by the authors.² For all experiments, we utilized the provided hyperparameters for IQ. To implement ILEED, we followed the codebase

provided by the authors, implementing the modified behaviour cloning loss alongside the IQ implementation.³ For IRLEED, we built on top of the aforementioned IQ implementation by adding a learnable parameter β_i , and an additional critic network ϵ_i , for each demonstrator i . This way, we sampled suboptimal policies according to: $\pi_i(a|s) \propto \exp(\beta_i(Q(s, a) + \alpha\epsilon_i(s, a)))$. All three methods utilized the same architecture for the critic networks, and followed the original hyperparameters used for the IQ implementation. For ILEED, the critic network was used to compute action probabilities using a final softmax layer. For IRLEED and ILEED, β_i was initialized to the same inverse temperature parameter used in the IQ implementation, and the learning rate was set to $5e - 4$. For IRLEED, the additional critic networks $\epsilon_i(s, a)$ were initialized with the same procedure as the critic network $Q(s, a)$, utilized the same learning rate divided by 10, and utilized the scaling factor $\alpha = 0.01$. We trained all methods using 50,000 and 100,000 time steps for Cartpole and Lunar Lander, respectively. For evaluation, we utilized the final policy, sampling 300 episodes to measure the mean reward.

To create datasets for varying levels of *precision* and *accuracy*, we randomly generated 3 suboptimal policies according to $\pi_i(a|s) \propto \exp(\beta_i(Q(s, a) + \alpha\epsilon_i(s, a)))$, where $Q(s, a)$ was a pretrained critic network provided by the original IQ implementation, and $\epsilon_i(s, a)$ was a randomly initialized critic network. For Cartpole, we utilized $\alpha = 0$ and $\alpha = 20$ for the high and low *accuracy* settings, respectively. For Lunar Lander, we utilized $\alpha = 0$ and $\alpha = 0.2$ for the high and low *accuracy* settings, respectively. For the low *precision* setting, β_i was sampled from a uniform distribution between 0 and 1 for Cartpole, and between 0 and 100 for Lunar Lander. For the high *precision* setting, the effect of β was removed and the policies were sampled according to the maximum state action values: $\pi_i(a|s) = \max(Q(s, a) + \alpha\epsilon_i(s, a))$. We ran this experiment in both the online and offline setting, comparing the performance of IRLEED, IQ, and ILEED, using 30 seeds for each dataset setting.

A.3. Atari with Human Data

As aforementioned, the implementation for the Atari experiments in Section 5.3 was identical to the one described above in Appendix A.2. For training, we utilized 1,000,000 time steps for all methods. For IRLEED, we did not update the error critic networks $\epsilon_i(s, a)$ or the temperature parameters β_i for the first 300,000 timesteps. For evaluation, we sampled 10 episodes from the policies recovered during the last 5 epochs of training, where each epoch corresponded to 5,000 time steps.

The two datasets used are publicly available, where dataset

²<https://github.com/Div99/IQ-Learn>

³<https://github.com/Stanford-ILIAD/ILEED>

A: simulated data using a pretrained expert policy, was provided alongside the original IQ implementation (Garg et al., 2021) and dataset *B*: collected data using adept human players, was part of a larger human study (Kurin et al., 2017). For Space Invaders, dataset *A* contained 5 trajectories with an average return of 1285, whereas dataset *B* contained 5 trajectories with an average return of 1801. For Qbert, dataset *A* contained 10 trajectories with an average return of 14760, whereas dataset *B* contained 10 trajectories with an average return of 17340. We ran this experiments using the three combinations of these datasets, averaging our results over 5 seeds.

A.4. Computational Resources

All of the experiments were performed on an internal cluster containing the 20C/40T Intel Xeon Silver 4114 CPU, 64GB RAM, and 4×GTX-1080 GPUs. Obtaining results for the Gridworld experiment with 121 datasets, each with 100 seeds, took roughly 3 days. Obtaining results for the simulated control tasks, Cartpole and Lunar Lander, took roughly 4 days each. Training models on the Atari environments took 40 hours per seed for IQ and IRLEED, and 20 hours per seed for ILEED.